Aerosol Extinction Coefficient Variations with Altitude at 3.75 μm in a Coastal Marine Environment

H. G. HUGHES

Electromagnetic Propagation Division, Naval Ocean Systems Center, San Diego, CA 92152

(Manuscript received 16 July 1979, in final form 13 April 1980)

ABSTRACT

Aerosol size distributions and meteorological parameters measured with altitude in a marine environment off the Southern California coast are presented. Extinction coefficients for a wavelength of 3.75 μm are calculated from Mie theory using the measured distributions and compared with those calculated using empirical models of aerosol size distributions which require as inputs the measured meteorological parameters.

1. Introduction

Analytical models of aerosol size distributions based on measurable meteorological parameters are of primary importance in the prediction of electro-optical systems performance at sea where transmission or particle size measurements cannot be easily made. Given the appropriate analytical model of the size distribution and the effective index of refraction of the aerosol, extinction coefficients at the wavelengths of interest can be calculated using Mie theory. Barnhardt and Streete (1970) provided a two-component (continental and maritime) analytical aerosol size distribution from which infrared (IR) extinction coefficients can be calculated. The continental component is described by a Junge (1955) power-law distribution and the maritime component is described by the modified gamma function used by Deirmendjian (1969). Included in the model are the effects of relative humidity on the size distribution and refractive indices of the aerosols. Not included in the model are the effects of surface wind velocity and the variation of the distributions with altitude.

More recently, empirical models have emerged which include the effects of surface wind speed and altitude dependencies (Selby *et al.*, 1976; Wells *et al.*, 1977). In the model of Selby *et al.* (hereafter referred to as the LOWTRAN 3B maritime model) the continental and maritime components are represented by log-normal distributions with the maritime component contributing 75% of the extinction at 0.55 μm. While the relative humidity and wind speed are not explicit to the model, the distribution is supposed to correspond to a relative humidity of 80% and moderate wind speeds. In the LOWTRAN 3B approach, the particle size distribution is assumed to be constant with altitude and the aerosol extinction coefficients as a function of wavelength are precalculated using the "oceanic" indices of refraction and then normalized to an observed surface visibility of 23 km which includes the contributions from Rayleigh scattering. The total number density of particles is allowed to vary exponentially with altitude from a value at the ground based on surface visibility. This procedure allows the extinction coefficient variation with altitude to be scaled from surface visibility measurements, but maintains a constant ratio of visible to IR extinction with altitude.

In the model of Wells *et al.* (hereafter referred to as the WGM model), the continental and maritime representations of Barnhardt and Streete are maintained as is the model of aerosol radius growth rate with relative humidity which assumes the dry particle to be NaCl. In the continental component, the constants of the Junge distribution were adjusted to agree with the work of Barnhardt and Streete for a relative humidity of 80% and a continental to maritime mixture ratio of 1:2.5. In the maritime component, the constants of the Deirmendjian distribution were modified to include surface wind speed and relative humidity based on fits to the empirical data of Manson (1965). Simple exponential scale heights were also introduced as functions of particle radius which (with relative humidity lapse rates) account for altitude variations. The aerosol size distribution model is normalized by a factor β^* (see Appendix) given by

$$\beta^* = \frac{3.912}{R_v \beta_{\text{cal}}(0.55\ \mu\text{m})}, \tag{1}$$

where R_v is the observed visibility at a single wave-

length $\lambda = 0.55$ μm and β_{cal} (0.55 μm) is the Mie aerosol extinction coefficient calculated for $\lambda = 0.55$ μm using the size distribution prior to normalization. In the original formalization, the contribution to extinction by Rayleigh scattering (which is inherent in the observed visibility) was not added to the calculated extinction coefficient in determining β^*. Also, if the visibility is measured by a transmission loss between a source and a receiver which has a finite bandwidth $\Delta\lambda$ the size distribution should then be normalized to the effective extinction coefficient measured over the bandwidth of the instrument given by

$$\langle \beta_{a+R} \rangle = \frac{1}{\rho} \ln \frac{\int_{\Delta\lambda} F(\lambda)W(\lambda) \exp\{-[\beta_a(\lambda) + \beta_R(\lambda)]\rho\} d\lambda}{\int_{\Delta\lambda} F(\lambda)W(\lambda) d\lambda}, \quad (2)$$

where $\beta_a(\lambda)$ and $\beta_R(\lambda)$ refer to the Mie extinction coefficient calculated with the un-normalized size distribution and the extinction coefficient due to Rayleigh scattering, respectively, and ρ is the optical path length. $W(\lambda)$ is the source intensity and $F(\lambda)$ is the spectral response of the receiver. For a given size distribution at the ground the ratio of visible and IR extinctions is then fixed. However, unlike the LOWTRAN 3B model, this ratio will change with altitude in a manner dependent on the particle growth with changes in relative humidity.

The equation describing the LOWTRAN 3B model is adequately described in the referenced article and will not be repeated here. However, it should be noted that in Eq. (12) of Wells *et al.* (1977) a constant factor of 2.3 incorrectly appears in the numerator of the marine component. This factor should be in the denominator and arises from the conversion of the distribution represented by $dN/d(\log r)$ (where N is the number of particles per unit volume with radii $\leq r$) to that of $n(r)$ (which is the number of particles per unit volume with radii between r and $r + dr$). Also the radius growth factor which appears in the denominator of Eq. (12) as a multiplying factor of both the continental and marine components should be the growth factor which is normalized to the 80% relative humidity data of Barnhardt and Streete (private communications, M. W. Munn). The corrected equation for the WGM model is described in the Appendix.

The empirical models have been developed from limited sets of surface measurements and their validity with altitude has not yet been examined. Measurements are presented here of aerosol size distributions with altitude which were obtained in a coastal marine environment off Southern California. In the following sections the aerosol measurements are discussed. Aerosol extinction coefficient variations with altitude calculated for a single wavelength using the measured size distributions are then compared to those calculated using the WGM and LOWTRAN 3B maritime aerosol models. This approach (requiring only single data point comparisons) is taken rather than comparing the individual number densities as a function at all altitudes. The contribution to extinction from scattering and absorption by atmospheric gases are not included in the calculations.

2. Measurements

During April–May 1978, measurements of aerosol size distributions were made in the vicinity of San Nicolas Island using an airborne Knollenberg ASSP-100 spectrometer probe. The spectrometer was mounted in the free-airstream on top of a twin engine Piper Navajo aircraft. The instrument sizes particles in four overlapping bands which are individually divided into 15 different radius intervals. Spectra were measured in each range band every second and digitally recorded on magnetic tape. The digitized data are subsequently processed by a Data General Corporation Nova 800 computer. Spectra in each range band are then combined to give a radius coverage from 0.225 to 14.7 μm for a 4 s time period.

Also, mounted on the aircraft are air temperature (HP200A quartz thermometer) and dew-point (EG&G TM 73-244) sensors, which (with digitization) allow the relative humidity to be calculated to within ±6% accuracy at 80% for an air temperature of 20°C. A pressure sensor provides elevation measurements to an accuracy of ±9 m and each meteorological parameter is digitally sampled every 5 s. The aircraft was flown at ~70 m s^{-1} on differing constant altitude radials away from the island so that measured size spectra represent 280 m horizontal distance. Vertical profiles of aerosol size distributions and meteorological parameters also were obtained by flying the aircraft in spiral ascents and descents of ~2 m s^{-1} at locations several nautical miles from the island. The surface visibilities required as inputs to the models were determined from one of the visible wavelength bands of a Barnes transmissometer which was operated over a 4.07 km path at the northwest end of San Nicolas Island. The combined filter and detector spectral response of the transmissometer band is centered at 0.55 μm and is nearly identical to the CIE (International Commission on Illumination, Paris 1948) photopic response with 50% power transmission points at 0.55 and 0.61 μm and

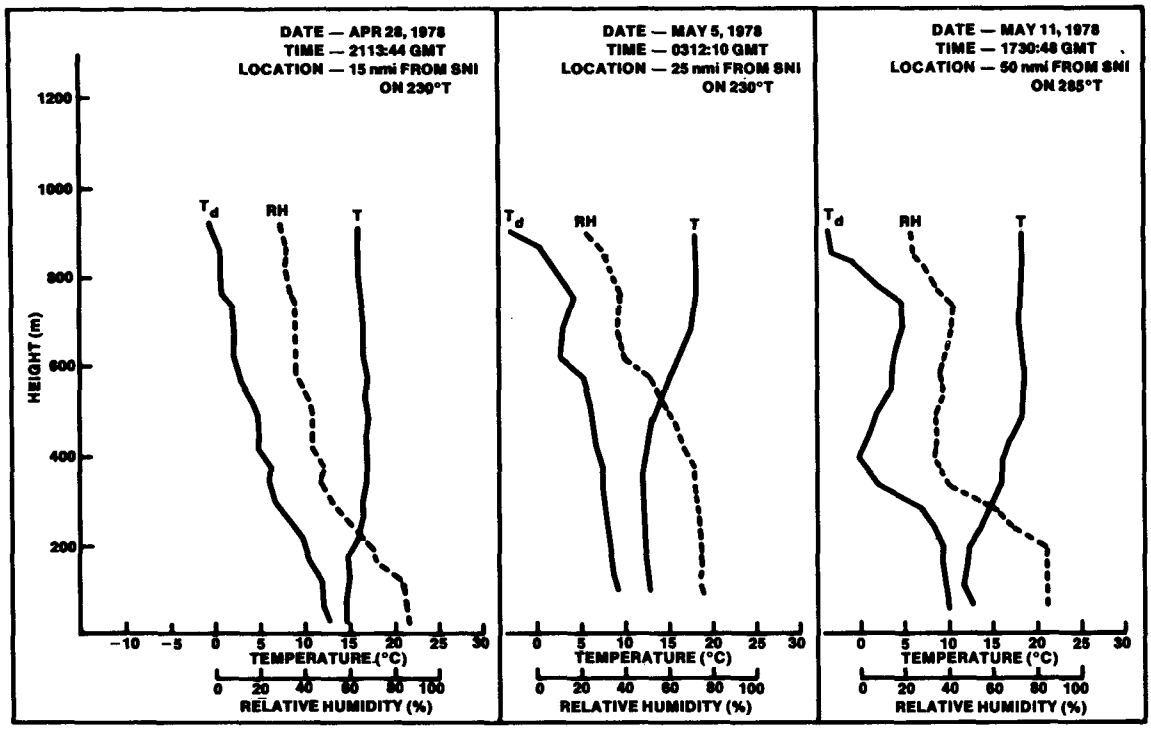

FIG. 1. Air (T) and dew-point (T_d) temperature measured at sea as a function of altitude from which the relative humidity (RH) profiles are calculated.

1% power transmission points at 0.3 and 0.825 μm. The Rayleigh extinction coefficients required as inputs to (2) to evaluate the WGM were determined from the expression of McClatchey and D'Agati (1978) given by

$$\beta_R(\lambda) = 2.94 \times 10^{-4}\, \lambda^{-4.0117}\left(\frac{P}{T}\right)\ [\mathrm{km}^{-1}], \quad (3)$$

where λ is the wavelength (μm), and P and T are the atmospheric pressure (mb) and temperature (K), respectively. For the calculations, the surface pressure and temperature were measured at the transmissometer location. The surface wind speeds over the ocean were also estimated from wind measurements at the transmissometer receiver location.

To calculate the aerosol extinction coefficients β_a from the measured distributions the integral

$$\beta_a = \pi \int_{r_0}^{r_1} r^2 n(r) K_e\left(\frac{2\pi r}{\lambda}, \epsilon\right) dr \quad (4)$$

is numerically evaluated. In Eq. (1), $n(r)$ is the measured number of particles per unit volume having radii between r and $r + dr$. K_e is the total cross section for extinction determined by the Mie theory and normalized to the spherical particle geometrical cross section. ϵ is the complex index of refraction at a wavelength λ. For the calculations here, the "oceanic" refractive indices of LOWTRAN are utilized. Actually, (1) is integrated by using Simpson's rule over unequally spaced intervals. A third-order polynomial fit is used to interpolate the measured distributions between the radius interval midpoints to fit the size parameters for which the Mie coefficients are given.

To compare extinction coefficient variations with altitude, data acquired during flights at sea away from the island on three different days are presented. For these days, the air (T) and dew-point (T_d) temperatures measured as a function of altitude, from which the relative humidity (RH) profiles were calculated, are shown in Fig. 1. The data were acquired during spiral ascents at the locations and times shown in the figures. The surface wind speeds (V_s) were 3–5, 5–7 and 10–12 m s^{-1} and the surface visibilities were 16, 11 and 23 km for 28 April, 5 and 11 May, respectively. The data chosen represent (i) a shallow mixed layer below a weak temperature inversion (28 April), (ii) a deep mixed layer below a strong temperature inversion (5 May), and (iii) a shallow mixed layer below a strong temperature inversion (11 May). On 28 April and 5 May, several flights of 5–7 min duration were made on different constant altitude radials away from the island. The longer duration constant altitude flights allow a more accurate sampling of the larger particles than do the spiral flights.

3. Comparison of models with measurements

In Fig. 2, the aerosol size distribution measured during one of the 5 May constant altitude flights is compared with the WGM model. The measured

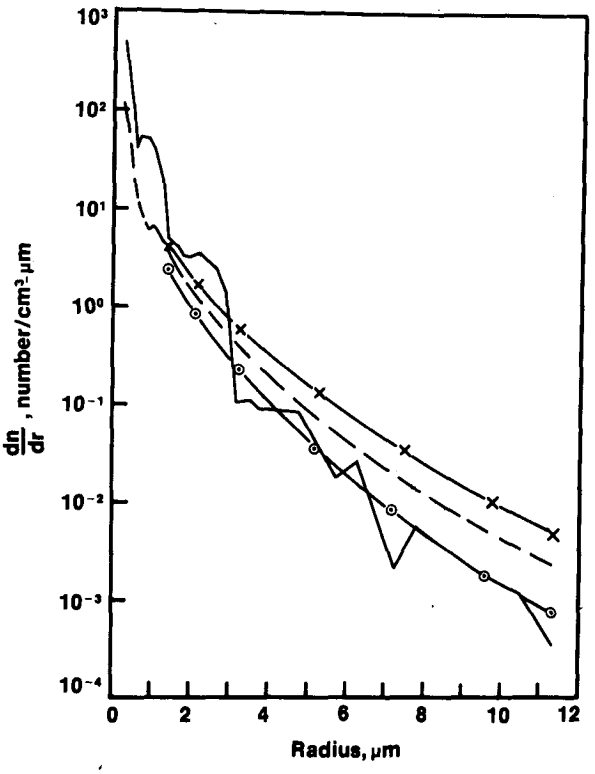

FIG. 2. Comparison of aerosol size distributions measured (——) at sea on 5 May 1978 during a constant altitude flight at 138 m and those calculated using the WGM model for V_s = 9 m s^{-1}, RH = 74% (○ —— ○); V_s = 11 m s^{-1}, RH = 80% (— —); and V_s = 13 m s^{-1}, RH = 86% (× —— ×).

spectrum represents a 5 min and 21 s sampling time at 138 m altitude during which the average humidity along the flight path was 80%. The model distributions were calculated at radii corresponding to the Knollenberg channel midpoints using the measured relative humidity and wind speed of 11 m s^{-1} and for the upper and lower values to be expected due to uncertainties in relative humidity and wind speed of ±6% and ±2 m s^{-1}, respectively. The scale heights used in the calculations were obtained from linear extrapolation of the values tabulated in the Wells *et al.* (1977) at 0 and 1 km. For particle radii ≥ 3 μm the lower distribution (corresponding to 74% and 9 m s^{-1}) is in better agreement with the measurements. For radii ≤ 3 μm the model is less sensitive to the changes in relative humidity and wind speeds. The uncertainties in humidity and wind are more likely to affect extinction coefficient calculations for the far-IR than for the visible and mid-IR wavelength bands. The small number densities of particles with radii near 10 μm also make extinction coefficient calculations for the far-IR bands unreliable. Ambiguities in the theoretical Mie scattering response of the ASSP-100 probe can cause some uncertainties in particle sizing below about 5 μm. This (as well as the neglect of particles < 0.225 μm) can cause uncertainties in calculated extinction coefficients for the visible and (to a lesser degree) the mid-IR wavelengths. In work published elsewhere (Hughes and Richter, 1980), a comparison was made of low-level aerosol extinction coefficients determined from the Barnes transmissometer at SNI and the aircraft Knollenberg probe which was flown along the propagation path. For the visible and far-IR bands the Knollenberg values were factors near 4 larger than the transmissometer. While uncertainties are also to be expected in the transmission measurements, the Knollenberg and transmissometer best agreed to within factors of 1.5 to 2 in the mid-IR band (50% power transmission points of 3.7 and 3.9 μm). For this reason, a wavelength of 3.75 μm is selected to compare the calculated and modeled extinction coefficient variations with altitude.

In Fig. 3 the extinction coefficients calculated with altitude using aerosol size distributions measured 28 April during constant altitude flights and a spiral ascent are compared with the models. There are considerable fluctuations with altitude in the extinctions determined from the spiral ascent data. However the trend of the variation with altitude closely follows the constant altitude data. Similarly in Figs. 4 and 5, extinction coefficient variation compared using the measurements of 5 and 11 May, respectively (data from constant altitude flights were not available on 11 May). In the three data sets, the models agree within a factor of 2 or better

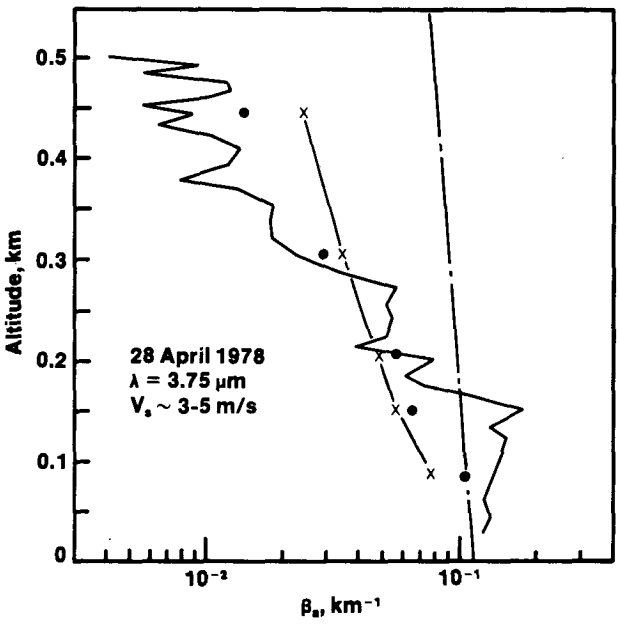

FIG. 3. Aerosol extinction coefficient variation with altitude calculated using aerosol size distributions measured during constant altitude (●) and spiral (——) aircraft flights; the WGM model (× —— ×); and the LOWTRAN 3B maritime model (— · —).

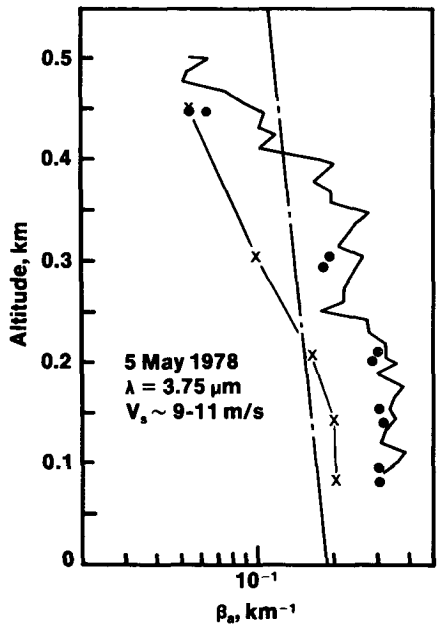

FIG. 4. As in Fig. 3.

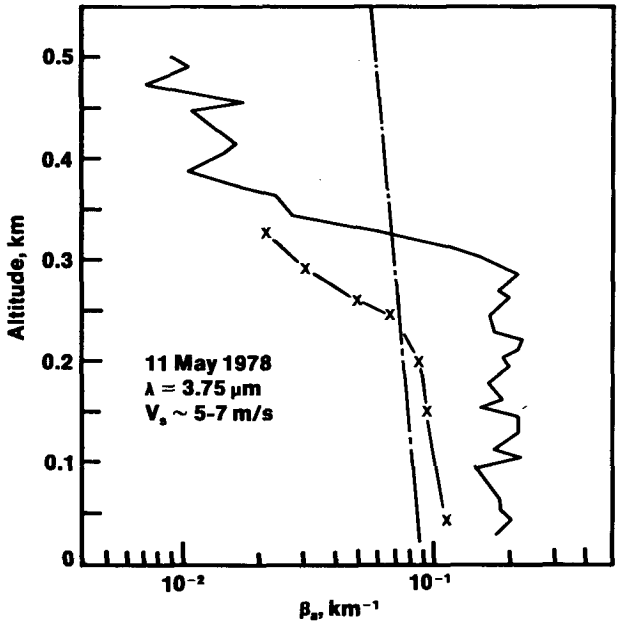

FIG. 5. As in Fig. 3 except measured during a spiral aircraft flight (——); the WGM model (× —— ×); and the LOWTRAN 3B maritime model (— - —).

with the Knollenberg data at low altitudes within the mixed layers. This is good agreement allowing for similar uncertainties in the Knollenberg-transmissometer comparisons.

4. Discussion

There appears to be little advantage to the WGM model over the LOWTRAN 3B model at low altitudes within the mixed layers for the visibilities and wavelength considered here. The major difference between the measurements and models occurs with the variation in extinction coefficient with altitude above the mixed layers. This is especially evident in the 11 May data of Fig. 5 where there was a strong temperature inversion above the mixed layer which gave rise to a strong relative humidity gradient between 200 and 400 m. The WGM model lapse rates follow better the Knollenberg data lapse rates than does the LOWTRAN 3B model which is simply scaled exponentially with altitude. For these types of temperature inversions, where long slant path ranges at sea are of interest, the users of LOWTRAN 3B stand the risk of underestimating the range at which a fixed transmittance will occur. The extinction calculations from both measured and modeled distributions were made assuming the aerosol index of refraction to be invariant with particle size and altitude. If this were not the case it could account for some of the differences between the measured and modeled values.

In Figs. 3, 4 and 5 the aerosol extinction coefficient variations with altitude are nearly constant within the mixed layer and are similar to the corresponding relative humidity lapse rates in Fig. 1. Although there appears to be good correlation between humidity and extinction, the relationship differs with each data set. This is seen in Fig. 6 where the average extinction coefficient calculated from size distributions measured during the constant altitude flights of 28 April and 5 May are plotted versus the average measured value of saturation ratio (relative humidity divided by 100) at each altitude. In the figure, the regression analyses

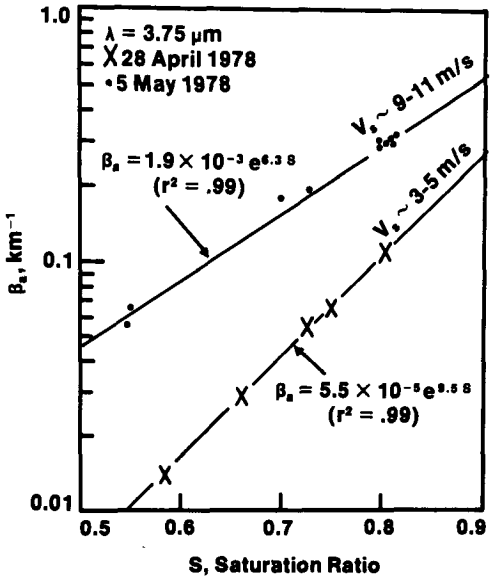

FIG. 6. Aerosol extinction coefficients calculated from aerosol size distributions measured at sea during constant altitude flights versus the average value of saturation ratio measured during each flight.

(r^2 = coefficient of determination) indicate different exponential dependencies between aerosol extinction and humidity for the two days. While a relationship between humidity and extinction is recognized (Hänel, 1976), it depends almost exclusively on the chemical composition of the dry particles for relative humidities less than 95%. There is evidence that the differing relationships between extinction and humidity found here most probably result from the differing air mass characteristics for the two days. Air trajectory analyses (Rosenthal *et al.*, 1979) based on satellite and synoptic meteorological data has shown that on 28 April the circulation causing air transport to San Nicolas Island was from the land to sea or continental, while on 5 May the air arriving at the island was of a mixed maritime and continental origin.

The work of Wells *et al.* (1977) was a first attempt to model IR extinction coefficients as a function of sea surface wind speed and relative humidity. The data presented here indicate that the air mass history and its boundary-layer stability are factors which should be included in empirical models relating aerosol size distributions to meteorological parameters.

Acknowledgments. The author wishes to acknowledge the help of Dr. D. R. Jensen who was responsible for the Knollenberg measurements and Dr. J. H. Richter for many helpful discussions. Funding was provided by the Naval Material Command, Technology Division, under Program Element 62759N, Project F52551 and Task Area ZF52551002.

APPENDIX

Formulation of WGM Aerosol Size Distribution Model

The corrected equation describing the WGM model is

$$n(r) = \frac{\beta^*}{F'}\left\{0.47\left(\frac{r}{F'}\right)^{-4}\exp(-h/hc) + 0.434\alpha(C_1 + C_2V_s^{\delta}) \times \left(\frac{r}{F'}\right)\exp\left[-8.5\left(\frac{r}{F'}\right)^{\gamma} - h/hm\right]\right\}, \quad (1)$$

where

$n(r)$	number of particles cm^{-3} μm^{-1} (radius)
r	radius (μm)
h	altitude (km)
h_c, h_m	scale heights (km) for the continental and marine components, respectively (listed in tabular form as a function of particle radius and altitude in Wells *et al.*, 1977)
α	continental to maritime mixing ratio
F	radius growth factor [$=1 - 0.9\ln(1 - S)$ for $S \geq 0.4$]
S	saturation ratio
F'	$F(S)/F(0.8)$
V_s	surface wind speed (m s^{-1})

$$(C_1 + C_2V^{\delta}) = \begin{cases} 250 + 750V_s^{1.16}, & V_s < 7 \text{ m s}^{-1} \\ 6900V_s^{0.29}, & V_s \geq 7 \text{ m s}^{-1} \end{cases}$$

$$\gamma = 0.384 - 0.00293V_s^{1.25}$$

$$\beta^* = \frac{3.912}{R_v\beta_{\text{cal}}(0.55\ \mu\text{m})}.$$

REFERENCES

Barnhardt, E. A., and J. L. Streete, 1970: A method for predicting atmospheric aerosol scattering coefficients in the infrared. *Appl. Opt.*, **9**, 1337–1344.

Deirmendjian, D., 1969: *Electromagnetic Scattering on Spherical Polydispersions*. Elsevier, 77 pp.

Hänel, G., 1976: *Advances in Geophysics*. Vol. 19, Academic Press, 73 pp.

Hughes, H. G., and J. H. Richter, 1980: Extinction coefficients calculated from aerosol size distributions measured in a marine environment. *Opt. Eng.* (in press).

Junge, C., 1955: The size distribution and aging of natural aerosols as determined from electrical and optical data of the atmosphere. *J. Meteor.*, **16**, 654–659.

McClatchey, R. A., and A. P. D'Agati, 1978: Atmospheric transmission of laser radiation: Computer Code LASER. AFGL-TR-0029.

Manson, J. E., 1965: *Handbook of Geophysics and Space Environments*. McGraw-Hill, 5–22.

Rosenthal, J., T. Battalino and V. R. Noonkester, 1979: Marine/continental history of aerosols at San Nicolas Island during CEWCOM-78 and OSP III. Pacific Missile Test Center Tech. Publ. TP-79-33.

Selby, J. E. A., E. P. Shettle and R. A. McClatchey, 1976: Atmospheric transmittance from .25 to 28.5 μm: Supplement LOWTRAN 3B. AFGL-TR-76-0258.

Wells, W. C., G. Gal and M. W. Munn, 1977: Aerosol distributions in maritime air and predicted scattering coefficients in the infrared. *Appl. Opt.*, **16**, 654–659.